Turkish Journal of Electrical Engineering & Computer Sciences

http://journals.tubitak.gov.tr/elektrik/

Research Article

Turk J Elec Eng & Comp Sci
(2022) 30: 216 – 232

doi:10.3906/elk-2103-15

A novel energy consumption model for autonomous mobile robot

Gürkan GÜRGÖZE[1,*], **İbrahim TÜRKOĞLU**[2]
[1]Department of Software Engineering, Institute of Science, Fırat University, Elazığ, Turkey
[2]Department of Software Engineering, Faculty of Technology, Fırat University, Elazığ, Turkey

Received: 03.03.2021 • **Accepted/Published Online:** 29.09.2021 • **Final Version:** 19.01.2022

Abstract: In this study, a novel predictive energy consumption model has been developed to facilitate the development of tasks based on efficient energy consumption strategies in mobile robot systems. For the proposed energy consumption model, an advanced mathematical system model that takes into account all parameters during the motion of the mobile robot is created. The parameters of inclination, load, dynamic friction, wheel slip and speed-torque saturation limit, which are often neglected in existing models, are especially used in our model. Thus, the effects of unexpected disruptors on energy consumption in the real world environment are also taken into account. As a result, a prediction success rate of 98.56% was achieved. It has also been compared with existing energy models. It was found to give 2%–6% better results than existing energy models. Finally, the effects of the parameters used in the proposed model on energy consumption were revealed in an 8-state simulation study. These dynamics have been found to have significant effects on energy consumption

Key words: Energy model, energy consumption, mobile robot system model, slope, wheeled slip

1. Introduction

Mobile robots have started to be widely used in many areas of life with their developing hardware structures and artificial intelligence. Their widespread use has brought many problems with completing tasks[1, 2]. One of them is that they have sufficient autonomous energy source to ensure the continuity of movement and mission planning. Because not having enough energy will cause long-term or high-powered tasks to not be performed as planned [3, 4]. In this sense, many power supply studies and energy supply strategies have been developed for mobile robots such as the use of short-term batteries, use of renewable energy sources, hybrid power structures, charging tasks. However, the difficulties of their development and the inability to fully meet the increasing energy demand made the efficient use of the available energy in the mobile robot important [3, 5, 6]. In this regard, researchers have put forward many optimization methods and algorithms that take into account the internal and external dynamics that exist during the movement in order to use energy efficiently. When we look at the relevant studies, the issues of creating the most suitable shortcuts, speed control, position control, synchronous operation of hardware units, planning of movement patterns, motion controls, powerful task planning and energy consumption cost models come to the fore. However, in these studies, subject-specific limited energy cost models were generally used [2, 7–10]. For example, Tokekar et al. [11] and Kim et al. [12] aimed to find energy efficient speed values to ensure the motion of dc motors at optimum angular speeds. For this purpose, an energy cost model based on DC motor parameters has been created. Ganganath et al. [4] and Wallace et al. [13]

*Correspondence: gurkangurgoze@gmail.com

found energy efficient roads in rugged lands with an estimated energy cost model. Hari Maghfiroh et al. [14, 15] worked on energy efficiency with speed control algorithms. Li et al. [3] they presented an intuitive task planning method to use energy efficiently in multiple mobile robots . These constrained energy models do not fully reflect the real-world energy consumption information of the targeted movement or task. Because some internal (such as electronic structure, heat, internal friction) and external parameters (such as load, ground friction, slope, wheel slips) have been ignored in order not to go out of focus of the subject. Experimental environments were created according to conditions specific to the subject. Incomplete energy consumption information will also reduce the endurance of movements and tasks based on energy management. Because in reality, there are many factors that affect energy consumption during movement. This problem has led researchers such as Linfei Hou et al. [16], Morales et al. [17], Wahab et al. [18] and Jaramillo et al. [19] to study detailed energy models that consider all factors with a holistic approach. Among these, it has been determined that the parameters of slope, load, dynamic friction, maximum cycle speed, torque saturation, wheel slip and active passive status of sensors are generally neglected[2–19]. However, Jakub Čerkala et al.[20], Pellegrinell et al. [21], Yacoub et al.[22] etc. stated that these parameters neglected in their studies have effects on the traction force, speed and energy consumption of the system. For example, Wallace et al. [4], Guo et al. [23], Vidhya Prakash et al. [24], Tokaker et al. [11], Tian et al. [25], Khan et al. [26], Li et al. [27] stated that there are unexpected wheel slips due to ground and speed in the real world environment in mobile robots with differential drive. They revealed that these lateral shifts affect energy consumption. They stated that slip is generally neglected as it causes very little energy loss in the dynamic system, but it is a cost of moving away from the target distance and its effect on the speed of the mobile robot. There is also a longitudinal sliding. It occurs on sandy, muddy and icy roads. With the longitudinal slip, the mobile robots progress slows down and the motors run more than necessary. Thus, excessive energy consumption occurs. Neglecting the maximum speed or motor torque saturation causes unlimited energy consumption costs in the mobile robot system with the increase of speed. But, under normal conditions, motors have maximum speed saturation limits and limited energy consumption. The energy consumption of the system should not increase even if the speed and target distance increase after the mobile robot reaches saturation on straight, curved and downhill roads [23, 24, 28, 29]. In addition, usually, kinetic friction is used in system models. However, Jakub Čerkala et al. [20]. demonstrated in their friction model study that a mobile robot actually has a dynamic friction. It has shown that static friction and Stribek effects exist together with kinetic friction. In reality, the mobile robot must overcome a force caused by friction on the ground before it can move. This force is the traction force that occurs due to the static friction required for movement and consumes energy in the system. In addition, the Stribeck effect during movement affects energy consumption by ensuring that the transition from static friction to kinetic friction is made at minimum speed [30]. Continuous operation of sensors is taken into account in existing energy models. However, in some task planning studies, sensors are made active or passive according to the course of the task. Thus, energy savings are tried to be achieved by preventing unnecessary uses. Therefore, in the energy model proposed in this study, the active-passive state of the sensors was also taken into account. Thus, a more accurate energy consumption estimation is provided, suitable for all kinds of task planning [31, 32].

As can be seen, current energy models do not reflect the real energy consumption information of complex environments. This shows that there is a need for a complete energy model that reveals the energy consumption information taking into account the dynamics of the entire system. Therefore, in this study, a novel energy consumption model has been developed to complement the deficiencies of the current energy models. Especially the dynamic friction model, slope, maximum cycle speed, torque saturation, the availability of wheel slip and

sensor active-passive status parameters are the distinctive specificity of proposed energy model.

When we look at the parts of the article, the general structure and mathematical model of the mobile robot system are emphasized in the second part. In the third part, the new proposed energy model is mentioned. In the fourth chapter, in the light of all this information, simulation and experimental study of the energy model developed with various motion scenarios has been carried out. The performance of the energy model has been demonstrated by comparing it with other determined energy models.

Contributions of this article to energy model studies in mobile robots:

- In this study, a new predictive energy consumption model has been developed for mobile robot systems to facilitate the development of tasks based on efficient energy consumption strategies.
- For the proposed energy consumption model, a mathematical system model that takes into account all parameters during the motion of the mobile robot has been created.
- The effect of neglected components in the proposed energy model on energy consumption has been analyzed.

2. Mathematical model of the proposed mobile robot system

The performance of the mobile robot depends on performing the desired movement in the most accurate way. However, in order for the mobile robot to move correctly, the mobile robot system and its mathematical model must be set up correctly. Thus, the energy consumption information of the system components is obtained with the least error. The mobile robot system structure generally consists of path planning, position control, controller, dynamic analysis, kinematic analysis and trajectory smoothing components. Path planning is defined as obtaining the most appropriate and safe (collision avoidance) path according to static or dynamic obstacles in the movement area. Obtaining an optimal path brings the system closer to minimum consumption (energy, time etc.) and minimum error values (location, speed, distance, etc.). Especially, preventing unnecessary movements with road planning has an important effect on energy consumption [33, 34]. Another point in the motion planning of the mobile robot is that it can follow the given trajectory with the least error. This trajectory tracking is performed by position control algorithms. Thus, deviations from the targeted path are reduced and energy consumption is achieved. Trajectory tracking and position control is based on speed. In this case, there must be a speed controller component to move at the desired speed. Speed control in accordance with the dynamics of the environment will also prevent unnecessary accelerations or stops. This allows to control the energy consumption of the system [8, 15, 35, 36].

Correct position control is done with an accurate kinematics. Because kinematics shows us at which point we are in the field of motion and our next target point. As it is known, the mobile robot determines its position in the environment, target point and orientation parameters (orientation angle, linear velocity, angular velocity) primarily by kinematic analysis.

Differential mobile robots are generally used in mobile robot studies. The absence of lateral movements under normal conditions has made their use widespread. As shown in Figure 1a, these robots consist of two DC motors at the back and a free wheel at the front. Movement is realized by these DC motors. Therefore, the movement is performed relative to the rotation axis (robot coordinate plane) - Xr, Yr placed between the two wheels. In differential mobile robot systems, the center of gravity is taken at the midpoint (P) of the rotation axis as a structural design. Thus, the weight of the platform (m) is distributed equally on the two wheels and the effective weight becomes m/2. In this way, excessive calculations due to center of gravity shifts are eliminated.

However, in some differential mobile robot designs, the center of gravity (G) may shift by the distance "d" from the rotation axis (P). In this case, the distance of the center of gravity to the axis of rotation should be taken into account in the calculations. Under normal conditions, there is no lateral movement in differential driving mobile robots. Therefore, $V_y = 0$ and the resultant linear velocity becomes $V = V_x$.

$$V = V_x = \frac{(V_R + V_L)}{2} = \frac{(r.w_R + r.w_L)}{2}, V_y = 0 \ , \quad w = \frac{(V_R - V_L)}{2.l} = \frac{(r.w_R - r.w_L)}{2.l}, \dot{\theta} = \frac{d_\theta}{d_t} = w \tag{1}$$

V_R, V_L are right and left motor linear velocities, w_R, w_L are right and left motor angular velocities, w resultant angular velocity, θ angle, r is the radius of the wheel. The x and y coordinates of the point where the mobile robot is located:

$$\dot{x} = V.\cos\theta \ , \quad \dot{y} = V.\sin\theta \tag{2}$$

A nonholonomic differential drive mobile robot must meet the constraints in the following equation for correct motion according to its orientation and speed [37, 38].

$$\begin{gathered} \dot{x}.\sin\theta - \dot{y}.\cos\theta + \dot{\theta}.d = 0 \\ \dot{x}.\cos\theta + \dot{y}.\sin\theta + \dot{\theta}.l = r.w_R \\ \dot{x}.\cos\theta + \dot{y}.\sin\theta - \dot{\theta}.l = r.w_L \end{gathered} \tag{3}$$

However, the movement of mobile robots in real-time environments is not always ideal. Longitudinal and lateral shifts occur in mobile robots with the effect of ground and movement speed. Both cause undesirable distortion in the system's speed, angle and position. In other words, it causes the mobile robot to deviate from the way it should follow, causing speed and energy losses. The shifts especially affect the kinematic constraints. It is generally neglected as it has little effect on dynamic parameters. As seen in Figure 1b, F_{lt} force and V_{lt} speed affect the lateral movement of the mobile robot system. The kinematic equation of the mobile robot that takes into account the slip constraints is expressed as follows.

$$\begin{gathered} \dot{x}.\sin\theta - \dot{y}.\cos\theta + \dot{\theta}.d = V_{lt} \\ \dot{x}.\cos\theta + \dot{y}.\sin\theta + \dot{\theta}.l = r.(w_R - \mu_R) = V_R \\ \dot{x}.\cos\theta + \dot{y}.\sin\theta - \dot{\theta}.l = r.(w_L - \mu_L) = V_L \end{gathered} \tag{4}$$

$$\beta_{lt} = \arctan\frac{V_{lt}}{V}, s_i = \frac{r.\dot{\theta}_i - V_i}{V_i}, i = R, L \ , \quad \mu_R = (1 - s_R).w_R, \mu_L = (1 - s_L).w_L \tag{5}$$

μ_R, μ_L are angular velocities caused by longitudinal slipping of both wheels. s_R and s_L are the slip rates of the wheel depending on the speed during rotation. β_{lt} is the lateral slip angle of the wheels. At this point, it is assumed that information such as lateral velocity and angle of rotation are obtained by devices such as GPS, IMU or various methods such as Kalman algorithm. Because these subjects are a special field of study. Linear and angular velocities caused by longitudinal sliding during movement:

$$V_{LS} = \frac{r.(\mu_R + \mu_L)}{2} = \frac{r.(1 - s_R).w_R + r.(1 - s_L).w_L}{2} \ , \quad w_{LS} = \frac{r.(\mu_R - \mu_L)}{2.l} = \frac{r.(1 - s_R).w_R - r.(1 - s_L).w_L}{2.l} \tag{6}$$

The new coordinate information generated by wheel slip [25–27]:

$$\dot{x} = V.\cos\theta - V_{lt}.\sin\theta \ , \quad \dot{y} = V.\sin\theta + V_{lt}.\cos\theta \ , \quad \dot{\theta} = w \tag{7}$$

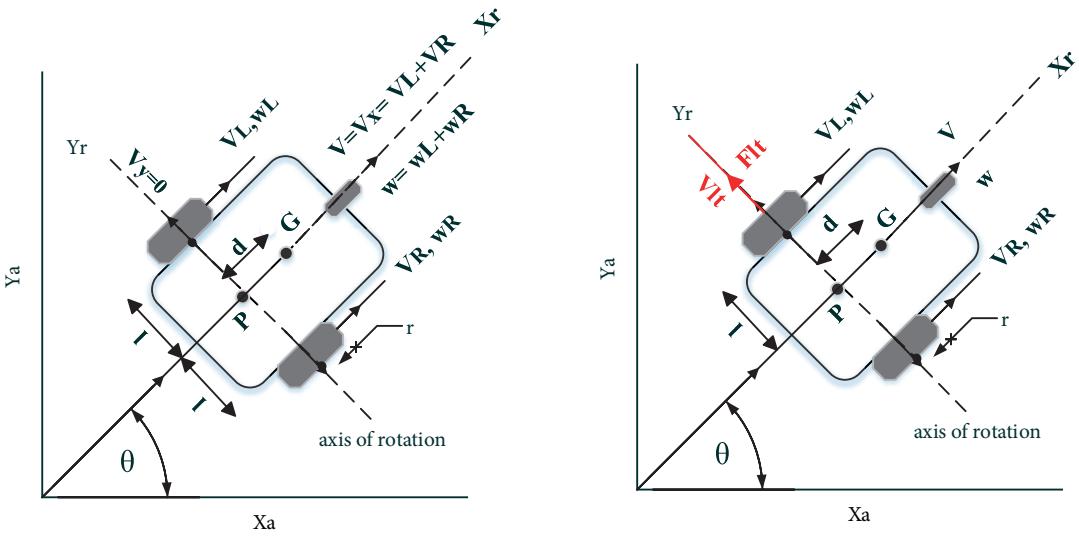

(a) In normal conditions

(b) Effect of lateral forces

Figure 1. Mobile robot motion axis and parameters.

A mobile robot performs its motion with independent DC motors. All internal and external factors affecting DC motors also affect the movement of the mobile robot. In order to perform the analysis of the system, the dynamic analysis of the mobile robot should be performed and its mathematical model should be obtained. The mathematical model consists of the DC motor model and the internal and external dynamics (environment dynamics) that affect it. The mathematical model of the DC motor is obtained as a transfer function as in Eq (8).

$$G_s(s) = \frac{w(s)}{V(s)} = \frac{K}{(L.s + R_a).(J_m.s + b_m) + K^2} \tag{8}$$

V(s) is the voltage given to the system, R_a armature resistance, L_a armature inductance, $K_t = K_e = K$ inductance constant, J_m motor inertia and b_m motor internal viscous friction[30, 36, 39]. In addition, in some studies, the ground friction affecting the system, the load of the platform and the slope are seen as important parameters for the simulation to give more realistic results. In studies where the effects of real world conditions (topography, friction, weather conditions, and energy consumption) are more pronounced, the effects of neglected load, friction, sloping and bumpy roads on movement have to be added. These forces affecting on the mobile robot system are as shown in Figure 2.

Mobile system force equation including these parameters:

$$F_M = F_L + F_E + F_Z \tag{9}$$

F_M is the total driving force, F_L, is total inertia force of mobile platform, F_E is the gravitational force of the inclined road, F_Z is the ground friction force. The effects of these forces are examined separately for each

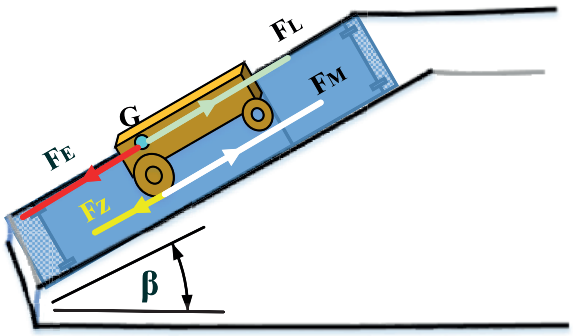

Figure 2. The effect of slope and friction forces.

motor. The differential mobile robot used in this study is designed so that its center of gravity is in the middle of the motion axis. Therefore, the effective weight applied by the mobile robot of mass m to each wheel is m/2. The general moment of inertia relative to the mass of the mobile robot platform:

$$F_L = \frac{m}{2}.a = \frac{m}{2}.\dot{V} = \frac{m}{2}.\dot{w}.r \tag{10}$$

β angle of slope. Gravitational force of the inclined road:

$$F_E = \frac{m}{2}.g.\sin\beta \tag{11}$$

Friction is the force against movement, as is known. Friction force consists of two parts as static and dynamic friction in mobile systems. Static friction (stiction) is friction at zero speed (v = 0) when the system is stationary. Kinetic friction is the friction when the system is activated (v! = 0). Static friction (stiction):

$$F_S = \mu_s.F_N.sign(v) \tag{12}$$

where $F_S = m.g$ or, for sloping ground $F_N = m.g.\cos\beta$ μ_s static friction coefficient, F_N denotes normal mass force acting on the robot, sign(v) motion direction.

The mobile robot has to overcome this F_S force in order to move. When the static friction is overcome, the mobile robot starts to move. However, this power is not immediately attained. Momentary traction force F_{TF} is produced in the motors until the F_S force is reached. This force acts as a static friction force in the mobile robot system until it reaches the F_S force. Therefore, the friction force acting is as follows.When the mobile robot starts moving, static friction leaves its place to kinetic friction. Kinetic friction is basically a viscous friction with coulomb friction. Coulomb friction is constant friction against movement that replaces static friction. While it is moving, the friction coefficient is μ_k. It is always $\mu_s > \mu_k$. Coulomb friction;

$$F_K = \mu_k.F_N.sign(v) \tag{13}$$

Viscous friction, on the other hand, is the friction applied by the ground to the wheels with rising speed. Coefficient of friction between ground and wheel b_z.

$$F_V = b_z.w \tag{14}$$

In addition, there is an effect of c_s coefficient that allows the system to pass with an increase in small speeds as it changes from static friction to kinetic friction. This effect is called the Stribeck effect.

$$F_{ST} = (F_S - F_K).e^{-c_s.|V|} \tag{15}$$

The kinetic friction thus formed;

$$F_{FZ}(V) = F_K + F_{ST} + F_V$$

$$F_{FZ}(V) = \mu_k.F_N.sign(v) + (F_S - F_K).e^{-c_s.|V|} + b_z.w \tag{16}$$

The friction model;

$$F_Z = \begin{cases} F_{TF}, & \text{for} \quad v = 0 \wedge F_{TF} < F_S \\ F_S.sgn(F_{TF}), & \text{for} \quad v = 0 \wedge F_{TF} \geq F_S \\ F_{FZ}(V), & \text{for} \quad v \neq 0 \end{cases} \tag{17}$$

Torque is the distance of the force acting on the system to the motor. T = force × distance, the distance is the radius of the wheel r. Accordingly, the total driving torque for the DC motor [20, 30, 39–42]:

$$T_m = T_L + T_E + T_Z \ , \quad T_m = F_L.r + F_E.r + F_Z$$

$$T_m = \frac{m}{2}.\dot{w}.r^2 + \frac{m}{2}.g.r\sin\beta + \mu_k.F_N.sign(v) + (F_S - F_K).e^{-c_s.|V|} + b_z.w \tag{18}$$

3. Proposed novel energy consumption model for mobile robot

The energy consumption of the mobile system consists of the energy consumption of the sensor, control and motor parts. In mobile robot studies, the power produced by the motor is considered as the power consumption of the system. Let us examine the energy consumption of these three parts. Constant energy consumption of the sensor part;

$$E_{sensor} = P_{sensor}.\triangle t \tag{19}$$

However, not all sensors are active in all cases. Some sensors are only active depending on the task or motion situation. Even in the moving environment, the amount of use of sensors increases according to the speed of the robot. Considering this, energy consumption according to the speed-active state dependent uses of the sensors;

$$E_{Sensor} = \begin{cases} \frac{1}{V_{max}} \int (v.P_{sensor}).d_t, & v > 0, V_{max} \quad \text{or} \quad w_{max} \\ 0, & v \leq 0 \end{cases} \tag{20}$$

If there is a constant energy consumption in the control part;

$$E_{control} = P_{control}.\triangle t \tag{21}$$

However, in reality, the energy consumption of the control part will also be different at the waiting, starting and continuous moment, even if it is a little. Energy consumption in this case;

$$E_{control} = \begin{cases} E_{standby} = P_{standby}.\triangle t \\ E_{startup} = \int (\phi.\triangle v + \frac{t^2}{10} + P_{standby}).d_t \\ E_{stable} = \int (P_{standby} + t^2).d_t \end{cases} \tag{22}$$

$P_{standby}$ is the power consumption at standby, ϕ is the energy factor given to start the controller, $\triangle v$ is the instantaneous speed change [16–19]. The energy consumed by the motor consists of four parts depending on the dynamics of the system. The energy required for the system to set in motion is the kinetic energy in motion, the frictional energy and the heat energy generated by the motion system. Generally, parts other than kinetic energy during motion are neglected or simply added to the system. However, for a more realistic energy consumption calculation, the dynamics affecting these four parts should be added to the system in the most accurate and complete manner. The power in the motors is as in Eq. 23 with the voltage provided by the source and the current drawn by the motor

$$P = V.I \tag{23}$$

At the same time, we can obtain the power consumed by the motor by multiplying the torque (T) of the motor and its angular velocity (w)[43].

$$P = T.w \tag{24}$$

The torque force generated by the motor against internal and external dynamics is derived as Eq. 18 in Section 2. With this torque force, the power and energy consumption of the motor is obtained as in Eq. 25 (for the mobile robot in motion). Thus, unlike other energy models, the effects of friction, load and slope on energy consumption are included in the system with the motor torque force.

$$T_m = T_L + T_E + T_Z$$

$$T_m = \frac{m}{2}.r^2.\frac{d^2\theta}{dt^2} + \frac{m}{2}.g.r\sin\beta + \mu_k.F_N.sign(v) + (F_S - F_K).e^{-c_s.|V|} + b_z.\frac{d\theta}{dt}$$

$$P_k = T_m.w \tag{25}$$

In energy consumption models, the power consumption limit of the motor is generally not taken into account. Because motors produce limited torque. This situation causes the energy cost of the motor to be more than necessary on straight roads, turns and descents. To prevent this, a limitation should be imposed on the maximum speeds (V_{max}, w_{max}) and maximum torque (T_{max}). In the turns, the maximum torque and speed values against the centrifugal force are taken into account in the studies. The maximum speed of the curved path is obtained as follows:

$$v = \sqrt{\frac{(e+\mu).g}{k}} \tag{26}$$

θ is the curvature angle, e =tanh(θ) curvature height, r is the radius of curvature, μ is ground friction, g is gravity, k=1/r. It is assumed that these values are obtained by various methods. Thus, on curved roads, deviations from the road are prevented and the energy consumption estimation is obtained more accurately [11, 28, 29].

$$P_{max} = T_{max}.w_{max} \quad P_{max} = F_{max}.v_{max} \tag{27}$$

$$P_k = \begin{cases} P_k, & v < v_{max} \quad \text{or} \quad w_{max} \\ P_{max}, & v \geq v_{max} \quad \text{or} \quad w_{max} \end{cases} \tag{28}$$

The amount of energy consumed by the motor against torques acting;

$$E_s = \int P_k.(t).d_t$$

$$E_s = \int T_m.(t).w.(t).d_t \tag{29}$$

The heat energy arising in the armature of the motor,

$$E_h = \int (\epsilon t_2 + \sigma.v + \lambda.t).d_t \tag{30}$$

Here ϵ and λ are heat time constant and σ is velocity heat constant. Consumed energy by the motor:

$$E_{motion} = E_s + E_h \tag{31}$$

Total energy consumption of the entire system;

$$E_{total} = E_{sensor} + E_{control} + E_{motion} \tag{32}$$

The Simulink connection created for power consumption on the transfer function is as shown in Figure 3 [16–21].

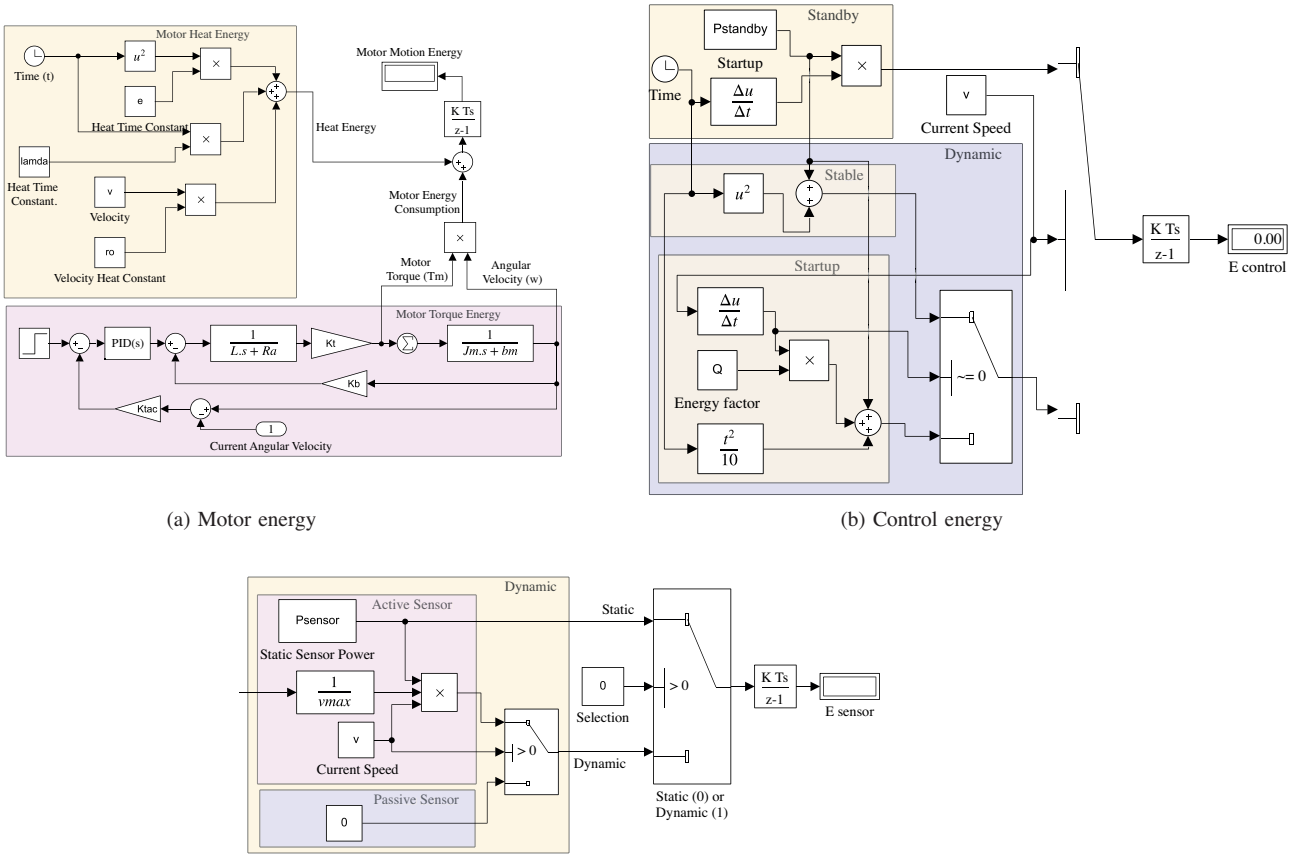

(a) Motor energy

(b) Control energy

(c) Sensor energy

Figure 3. Motor power consumption Simulink models.

4. Simulation and experimental results

4.1. Simulation and experimental results

An experimental study based on simulation and application was carried out to measure the performance of the energy model proposed in this section. Thus, a comparison of estimated and actual energy consumption information was made. First of all, the mobile robot system and energy model were created in the Simulink environment, taking into account the parameters of the physical mobile robot and the environment dynamics. The transfer function of the dc motor model required for the simulation environment according to the parameters in Table 1 was obtained as in Eq. 32. Parameters of the DC motor in the experimental study Gurkan et al. [44] was determined by his work [45].

Table 1. DC motor parameters.

Parameters	Symbol	Value	Unit
Torque constant	K_t	0.8693	Nm/A
Emf constant	K_e	0.8883	V_s/rad
Motor viscous friction	J_m	0.038	Kg/m^2
Motor viscous friction	b_m	0.00075	N-ms/rad
Motor viscous friction	R_a	53.94	NOhm
Armature inductance	L_a	1	μH
Ground friction	b_z	1	Nms/rad

Mobile robot transfer function:

$$G_s(s) = \frac{w(s)}{V(s)} = \frac{0.8693}{(1.s + 53.94).(0.038.s + 0.00075) + 0.8693^2} \tag{33}$$

The features of the mobile robot in used in the experimental study are length = 0.2, width = 0.2 m, load m = 0.8 kg, radius of the wheel = 0.03, l = 0.1. Speeds of the motor, maximum angular velocity (rad/s) - $w_{max} = \sim 22$, desired maximum linear velocity (m/s) - v_{max}, $= \sim 0.66$. In the study, the average speed of motion of the mobile robot was taken into account as V = 0.4 (m/s). The maximum voltage applied to the motors is 12V. The friction surface of the movement medium was chosen as stone, and the ground of the wheel sliding part was chosen as sand. Stone and sand ground static friction μ_s=1.0, stone ground coulomb friction coefficient μ_k=0.7, sand ground μ_k=0.50, velocity increase coefficient $c_s = 20$ was determined [46, 47].

Ground detection is a detailed research topic. In this study, it is assumed that the ground are known beforehand. Thus, it is aimed not to go beyond the focus of the subject. In the simulation and experimental studies, the ground on which the mobile robot is located and the change of the friction coefficients based on this were carried out according to the image and position information. The environment image has been converted to gray level according to color differences as in Figure 4. In the gray image obtained, the obstacles were grouped as black regions, and the ground as white and gray regions. The white area is the stone floor and the gray area is the sand floor. When the mobile robot enters these areas, the ground coefficients change within the program.

$$Performance = \frac{SimulationTotalEnergyConsumption}{ExperimentalTotalEnergyConsumption}.100 \tag{34}$$

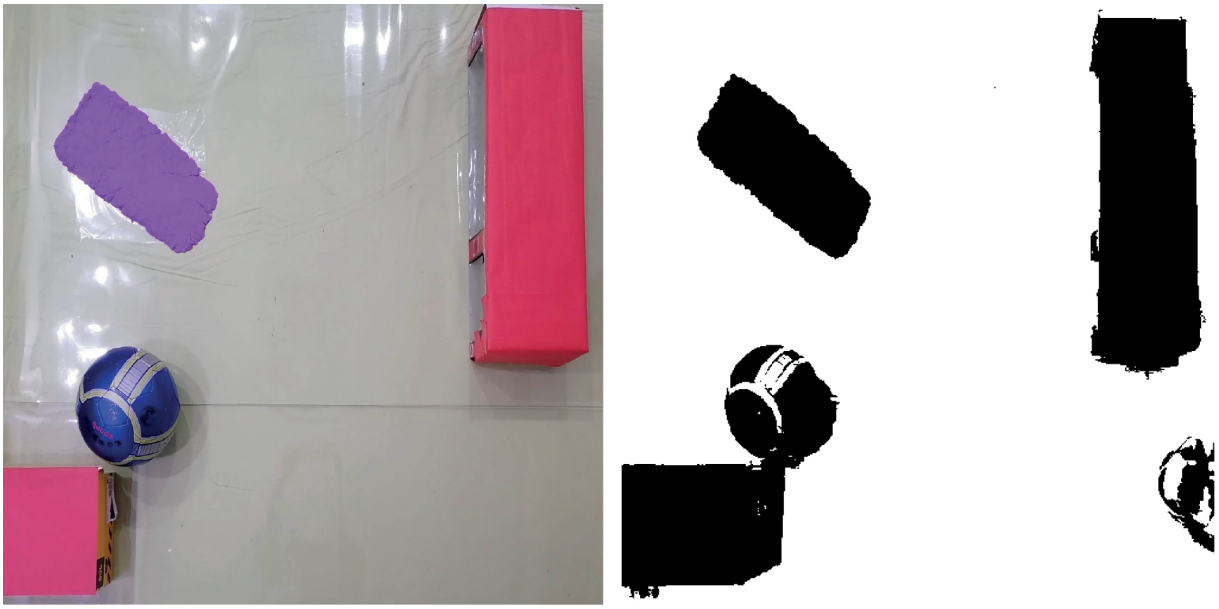

(a) Normal image (b) Gray image

Figure 4. Obtaining ground and obstacle information by image extraction.

An artificial potential field (APF) algorithm was used for path planning. This algorithm detects the obstacles in the environment and ensures reaching the target by avoiding collisions. At the same time, it can immediately respond to the dynamism of the environment. In the APF algorithm, the path planning is based on the thrust force of the obstacles and the pulling force of the target. Movement is carried out according to the net force obtained from pushing and pulling forces. The robot makes a move from the source to the target as if traveling up a valley [48]. Pure pursuit algorithm was used for route tracking. The algorithm is geometrically based. As is known, the obtained roads consist of movement points. The mobile robot sees the next point as the destination to the final destination. Pure Pursuit algorithm performs its movement to the next point by determining a human-like forward gaze distance until it reaches the target. The mobile robot adjusts its speed and orientation angle according to this forward gaze distance. For this reason, the forward view distance should be adjusted with the most appropriate value by trial and error in order not to miss the point or go by oscillation [49]. Parameters in pure pursuit algorithm were determined as look ahead distance (m) - 0.3, maximum angular velocity (rad/s) $w_{max} = \sim 20$, desired linear velocity (m/s) $v_{max} = \sim 0.6$. PID was used for speed control. PID parameters were obtained as $K_p = 10$ $K_i = 17.5$ and $K_d = 2.5$ using the Ziegler–Nichols frequency response method. As is known, energy measurement consists of sensor, control and motion parts. The mobile robot in this study has a camera as a sensor and a Raspberry pi 3 as a control card. $P_{sensor} = 1.2$ watts, $P_{control} = P_{standby} = 1.4$ watts and P $P_{startup} = 2.4$ watts were taken as actual operating values for the control card. Other necessary parameters such as temperature, rate constant, time constant are $\varphi = 0.7$, $\epsilon = 0.01$, $\sigma = 0.001$, $\lambda = 0.1$.

After the creation of the mobile robot system and the energy model, a common scenario was created for both test runs as in Figure 5. In the scenario, the road between 2 and 3 m on the route obtained by road planning was provided to be 7 % inclined and 3.5–4.5 meters of road distance to be sandy land. Lateral and longitudinal wheel slips occurred in sandy land.

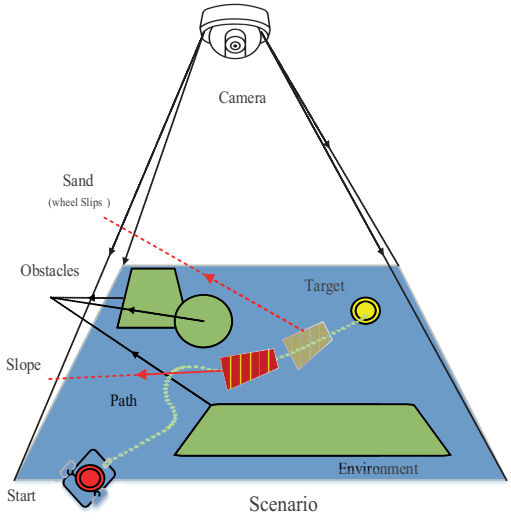

Figure 5. Scenario.

A physical environment suitable for the scenario determined for the experimental study was prepared as in Figure 6a. The physical mobile robot was integrated into the simulation environment. A road route was created with the Artificial Potential Field by taking the image of the environment. As a result, The energy consumption information was obtained using Eq. 23 according to the information received from the voltage/current sensors. Secondly, energy consumption information was obtained in the simulation environment using the same road plan as the proposed mobile robot system and energy consumption model as in Figure 6b.

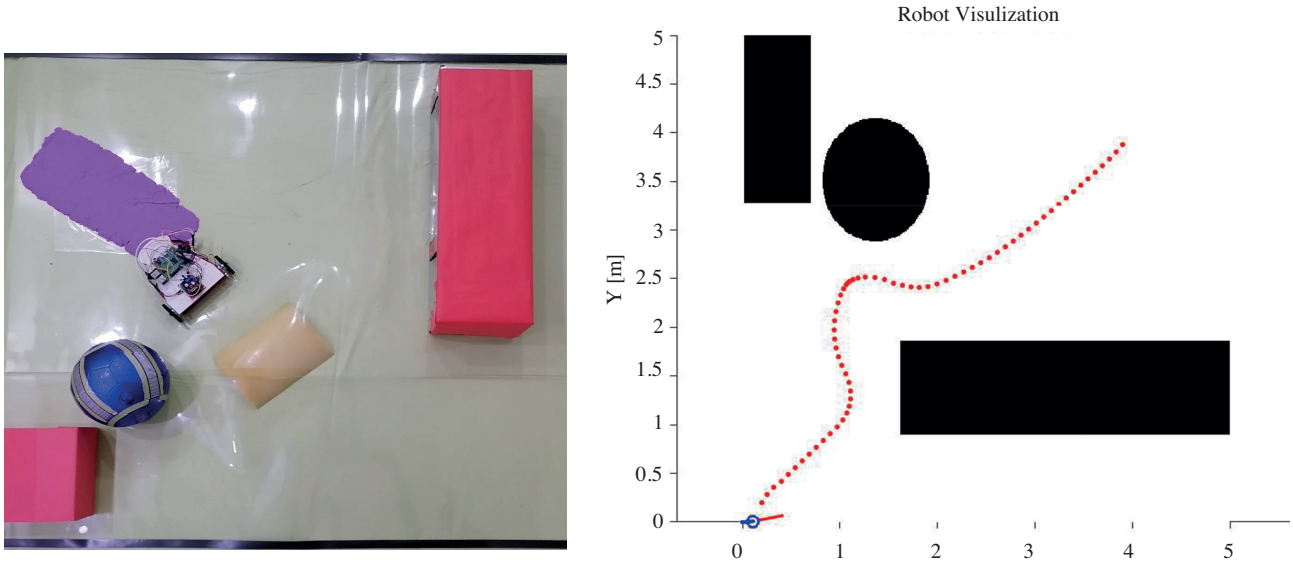

(a) Experimental

(b) Simulation

Figure 6. Energy consumption result.

4.2. Result and discussion

The performance of the energy consumption model proposed in Table 2 was 98.56% according to Eq. 33. Odometry errors occurred very little in the experimental study. Therefore, the time and distance values in the simulation and experimental study were considered equal.

Table 2. Energy consumption performance of proposed energy model.

Results	Time (s)	Dictance (m)	Total energy consumption
Simulation	24.5	6.43	1067.6
Experimental	24.5	6.46	1084.1

The parameters and performances used by some other developed energy consumption models in this field are presented in Table 3. It is seen in Table 3 that the energy model with the closest parameters to the proposed model is Jaramilo et al. [19]. The straight road energy consumption estimation of this energy model is 96.67%. Likewise, Wahap et al. [18] have an estimate of approximately 90% to 93% according to the energy consumption graph (model and actual measurement energy consumption comparisons between approximately 150 and 165) they stated in their studies. For Hou et al. [16], it was stated that there is approximately 3% difference between the proposed model and the experimental measurement [4, 17]. According to the parameters used and performance percentages, it turns out that our proposed energy model produces the closest estimate with 98.56% performance. It is seen that the proposed energy model gives 2%–6% more successful results compared to the existing energy models. In addition to these, as can be seen in Table 3, the environment parameters accepted by each energy model are different. Energy performance evaluations were made in an environment suitable for these parameters. However, the performance offered by the proposed energy model is according to the scenario in which all environment dynamics are present. If we take the estimated energy consumption of the current energy models in the scenario where all dynamics are present, the difference between the actual consumption result will be even greater according to the information in Table 4. Hence, the performance of existing energy models in complex environments will be lower than that shown in Table 3. This shows that the performance of the proposed energy model is higher than the performance of current energy models than that expressed in Table 3. For example, slope, electronics, wheel slip and temperature parameters are not available in the energy estimation model in the Jaramillo et al. study. The effects of parameters are ignored in the energy model proposed by Jaramillo et al. Performance measurements of the energy model were also made in experimental environments (no slope, ignoring electronic components) adapted to the developed energy model. Therefore, the performance values are high. However, in the examination in Table 4, it was seen that the slope (according to the angle of inclination) had an effect of 6%–9%, the control-sensor components (according to the number of sensors) had an effect of 3%–5% and the other components had an effect of 2%. In an environment where all environmental parameters are present, the performance of current energy models will decrease by 5%–10% [19].

At the same time, an 8-case application was carried out in a simulation environment on the current scenario to measure the effects of the parameters we use on energy consumption. A total of 0.5 kg load was added in the experiment.

As seen in Table 4, friction, load and slope parameters have significant effects on energy consumption. Especially on inclined roads, it is seen that the effect of friction increases with the effect of the load in the 6th

Table 3. Comparison of proposed energy models with existing models.

Energy models	Weight	Slope	Ground friction	Dynamic friction	Control-sensor	Wheel slips	Temperate	Performance (%)
Proposed model	✓	✓	✓	✓	✓	✓	✓	98.56
Hou et al. [16]	✓		✓		✓		✓	∼ 97
Wahab et al. [18]	✓		✓		✓			∼ 90–93
Jaramillo et al. [19]	✓		✓	✓				96.67

Table 4. Comparison of proposed energy models with existing models.

Cases	Weight	Slope	Ground friction	Dynamic friction	Control-sensor	Wheel slips	Temperate	Total energy consumption (j)
Case1	✓							814.2
Case2	✓	✓						822.9
Case3	✓	✓	✓					888.5
Case4	✓	✓	✓	✓				922.6
Case5	✓	✓	✓	✓	✓			932.8
Case6	✓	✓	✓	✓	✓	✓		988.2
Case7	✓	✓	✓	✓	✓	✓		1015.6
Case8	✓	✓	✓	✓	✓	✓	✓	1016.6

cases. Generally neglected wheel slips were found to be about 2%, and the energy consumed by dynamic friction was 1%. It has been observed that the sensor and control part consume energy that cannot be neglected. In order to examine the effect of the torque and speed saturation parameter of the mobile robot on energy consumption, the energy consumptions without speed limitation and with speed limitation was taken in the same scenario. In the simulation study including the previous speed limitation, the energy consumption was obtained as 1016.6 (J). Likewise, when the speed limit of the mobile robot is removed, the energy consumption obtained is 1028.7 (J). As can be seen, when the speed limits of DC motors are not specified, an unreal amount of energy consumption occurs. As can be seen in all these analyzes, there are many dynamics in the physical environment, and all of them have more or less effects. For a real consumption information, all parameters should be considered

5. Conclusion

In the article, a new energy consumption model has been developed to complement the shortcomings of current energy models. With this model, the energy consumption information of a mobile robot in the real environment is provided in the most accurate way. Thus, it is aimed to increase the durability of tasks based on energy management. In the next study, energy-oriented task and motion planning study that can adapt to the dynamics of the environment with the current energy model, system model and energy consumption analysis information of the components is aimed.

References

[1] Rozo L, Silverio J, Calinon S, Caldwell DG. Learning controllers for reactive and proactive behaviors in human–robot collaboration. Frontiers in Robotics and AI 2016;3:30.

[2] Patle BK, Pandey A, Parhi DRK, Jagadeesh A. A review: On path planning strategies for navigation of mobile robot. Defence Technology 2019; 15(4): 582-606.

[3] Li B, Moridian B, Kamal A, Patankar S, Mahmoudian N. Multi-robot mission planning with static energy replenishment. Journal of Intelligent and Robotic Systems 2019; 95(2): 745-759.

[4] Wallace N D, Kong H, Hill AJ, Sukkarieh S. Energy aware mission planning for WMRs on uneven terrains. IFAC-Papers OnLine 2019; 52 (30): 149-154.

[5] Plonski P A, Tokekar P, Isler V. Energy-efficient path planning for solar-powered mobile robots. Journal of Field Robotics 2013; 30 (4): 583-601.

[6] Angelina S, Afifah S, Susamti P, Priramadhi RA, Darlis D. Efficient energy consumption for indoor mobile robot prototype under illumination. In: Proceedings of the MATEC Web of Conferences; Bandung, Indonesia; 2018. pp. 11016-11019

[7] Gurguze G,Turkoglu I. Energy Management techniques in mobile robots. International Journal of Energy and Power Engineering 2018; 11(10): 1085-1093.

[8] Zakaria MA, Zamzuri H, Mamat R, Mazlan SA. A path tracking algorithm using future prediction control with spike detection for an autonomous vehicle robot. International Journal of Advanced Robotic Systems 2013; 10 (8): 309-317.

[9] Valero F, Rubio F, Llopis-Albert C. Assessment of the effect of energy consumption on trajectory improvement for a car-like robot. Robotica 2019; 37 (11): 1998-2009.

[10] Figurowski D, Jain A. Hybrid path planning for mobile robot using known environment model with semantic layer. In: AIP Conference Proceedings; Zakopane, Polond; 2018.pp.020014-020022.

[11] Tokekar P, Karnad N, Isler V. Energy-optimal trajectory planning for car-like robots. Autonomous Robots 2014; 37 (3): 279-300.

[12] Kim CH, Kim BK. Minimum-energy translational trajectory generation for differential-driven wheeled mobile robots. Journal of Intelligent and Robotic Systems 2007; 49(4):367–383.

[13] Ganganath N, Cheng CT, Chi KT. A constraint-aware heuristic path planner for finding energy-efficient paths on uneven terrains. IEEE transactions on industrial informatics 2015;11 (3): 601-611.

[14] Maghfiroh H, Ataka A, Wahyunggoro O, Cahyadi AI. Optimal energy control of dc motor speed control: Comparative study. In: International Conference on Computer, Control, Informatics and Its Applications (IC3INA); Jakarta, Indonesia; 2013. pp. 89-93.

[15] Maghfiroh H, Hermanu C, Ibrahim MH, Anwar M, Ramelan A. Hybrid fuzzy-PID like optimal control to reduce energy consumption. Telkomnika 2020; 18 (4):2053-2061.

[16] Hou L, Zhang L, Kim J. Energy modeling and power measurement for mobile robots. Energies 2019; 12 (1): 27-42.

[17] Morales MFJ, Mendoza JBG. Mixed energy model for a differential guide Mobile Robot. In: 23rd International Conference on Method and Models in Automation and Robotics (MMAR); Miedzyzdroje, Poland; 2018. pp.114-119.

[18] Wahab M, Rios-Gutierrez F, ElShahat A. Energy modeling of differential drive robots. In:Proceedings of the Annual IEEE SoutheastCon Conference; Fort Lauderdale, Florida; 2015.pp. 1-6.

[19] Jaramillo-Morales MF, Dogru S, Gomez-Mendoza JB, Marques L. Energy estimation for differential drive mobile robots on straight and rotational trajectories. International Journal of Advanced Robotic Systems 2020; 17 (2): 1729881420909654.

[20] Cerkala J,Jadlovská A. Nonholonomic mobile robot with differential chassis mathematical modelling and implementation in simulink with friction in dynamics. Acta Electrotechnica et Informatica 2015;15 (3):3-8.

[21] Pellegrinelli S, Borgia S, Pedrocchi N, Villagrossi E, Bianchi G et al. Minimization of the energy consumption in motion planning for single-robot tasks. In: The 22nd CIRP conference on Life Cycle Engineering (Procedia CIRP 29);Sydney, Australia ;2015. pp.354-359.

[22] Yacoub MI, Necsulescu DS, Sasiadek JZ. Energy consumption optimization for mobile robots motion using predictive control. Journal of Intelligent and Robotic Systems 2016; 83 (3):585-602.

[23] Guo J, Gao H, Ding L, Guo T, Deng Z. Linear normal stress under a wheel in skid for wheeled mobile robots running on sandy terrain. Journal of Terramechanics 2017;70:49-57.

[24] Vidhyaprakash D, Karthikeyan S, Periyasamy M, Kalaimurugan K,Navaneethasanthakumar S. Positioning of Two-wheeled mobile robot to control wheelslip by using the wheel rotate planning technique. Journal of Scientific and Industrial Research 2019;78: 879-884.

[25] Tian Y, Sarkar N. Control of a mobile robot subject to wheel slip. Journal of Intelligent and Robotic Systems 2014; 74 (3): 915-929.

[26] Khan H, Iqbal J, Baizid K, Zielinska T. Longitudinal and lateral slip control of autonomous wheeled mobile robot for trajectory tracking. Frontiers of Information Technology and Electronic Engineering 2015; 16 (2): 166-172.

[27] Li S, Ding L, Gao H, Chen C, Liu Z et al. Adaptive neural network tracking control-based reinforcement learning for wheeled mobile robots with skidding and slipping. Neurocomputing 2018; 283: 20-30.

[28] Tork N, Amirkhani A, Shokouhi SB. An adaptive modified neural lateral-longitudinal control system for path following of autonomous vehicles. Engineering Science and Technology, an International Journal, 2021;24 (1):126-137.

[29] Tokekar P, Karnad N, Isler V. Energy-optimal velocity profiles for car-like robots. In: 2011 IEEE International Conference on Robotics and Automation; Shanghai, China; 2011.pp.1457-1462.

[30] Singh AP, Narayan U, Verma A. Speed control of DC motor using PID controller based on matlab. Innovative Systems Design and Engineering 2013; 4 (6):22-28.

[31] MahmoudZadeh S, Powers DM, Sammut K, Atyabi A, Yazdani A. A hierarchal planning framework for AUV mission management in a spatiotemporal varying ocean. Computers and Electrical Engineering 2018; 67:741-760.

[32] Schwarzrock J, Zacarias I, Bazzan AL, DeAraujo Fernandes RQ, Moreira LH et al. Solving task allocation problem in multi unmanned aerial vehicles systems using swarm intelligence. Engineering Applications of Artificial Intelligence 2018; 72: 10-20.

[33] Bayat F, Najafinia S, Aliyari M. Mobile robots path planning: Electrostatic potential field approach. Expert Systems with Applications 2018; 100:68-78.

[34] Li B, Liu H, Su W. Topology optimization techniques for mobile robot path planning. Applied Soft Computing 2019; 78: 528-544.

[35] Patle BK, Parhi D, Jagadeesh A, Sahu OP. Real time navigation approach for mobile robot. Journal of Computers (JCP) 2017; 12 (2):135-142.

[36] Leena N,Saju KK. Modelling and trajectory tracking of wheeled mobile robots. Procedia Technology 2016; 24:538-545.

[37] Malu SK, Majumdar J. Kinematics, localization and control of differential drive mobile robot. Global Journal of Research In Engineering 2014; 14 (1):1-9.

[38] Zhang J, Wu Z,Lu S. Kinematic analysis, modeling and simulation of the substation inspection robot. In:3rd International Conference on Mechatronics, Robotics and Automation (ICMRA 2015); Shenzhen, China;2015. pp.681-689.

[39] Hirpo BD, Zhongmin W. Design and control for differential drive mobile robot. International Journal of Engineering Research and Technology (IJERT) 2017; 6 (10):327-334.

[40] Stepniewski A, Grudzinski J, Krzywicka M, Stankiewicz A. Dynamics model of a vehicle with DC motor. Teka Comission of Motorization an Energetics in Agriculture 2015; 15 (1):65-70.

[41] Lian C, Xiao F, Gao S, Liu J. Load torque and moment of inertia identification for permanent magnet synchronous motor drives based on sliding mode observer. IEEE Transactions on Power Electronics 2018; 34 (6): 5675-5683.

[42] Nouri BM. Modelling and control of mobile robots. In: Proceeding of the First International Conference on Modeling, Simulation and Applied Optimization (ICMSAO-05); Sharjah, United Arab Emirates (UAE);2005. pp.1-6

[43] Jaramillo-Morales MF, Dogru S, Marques L. Generation of energy optimal speed profiles for a differential drive mobile robot with payload on straight trajectories. In: 2020 IEEE International Symposium on Safety, Security, and Rescue Robotics (SSRR); Abu Dhabi, UAE; 2020.pp.136-141

[44] Gurgoze G,Turkoglu I. Development of experimental setup for determining the parameters of DC motors used in mobile robots. Journal of Polytechnic 2021; 1:1-9. doi:10.2339/politeknik.762077

[45] Patel H, Chandwani H. Simulation and experimental verification of modified sinusoidal pulse width modulation technique for torque ripple attenuation in Brushless DC motor drive. Engineering Science and Technology, an International Journal 2020; 24 (3):671-681

[46] Bahri R, Boucetta R, Naoui SBHA. A novel frictional force control of a wheeled robot. In: 2017 18th International Conference on Sciences and Techniques of Automatic Control and Computer Engineering (STA); Monastir, Tunisia ;2017.pp.229-234

[47] Lex C. Maximum Tire-Road Friction Coefficient Estimation.PhD, Verlag der Technischen Universität Graz,Austria,2015.

[48] Azzabi A, Nouri K. An advanced potential field method proposed for mobile robot path planning. Transactions of the Institute of Measurement and Control 2019;41 (11): 3132-3144.

[49] Samuel M, Hussein M, Mohamad MB. A review of some pure-pursuit based path tracking techniques for control of autonomous vehicle. International Journal of Computer Applications 2016; 135 (1):35-38.